Yaojia ZHANG, Master Degree (corresponding author)
zhangyaojia1219@foxmail.com
University of Shanghai for Science & Technology, Shanghai, China

Yan GAO, PhD
gaoyan@usst.edu.cn
University of Shanghai for Science & Technology, Shanghai, China

Adaptive Step-Size ADMM Based Real-Time Pricing Strategy for Smart Grids with Stepwise Carbon Trading Considerations

Abstract. *In the current pursuit of diversified energy complementation and a low-carbon economy, the operation of power systems faces unprecedented complexity. Real-time pricing (RTP) strategies based on demand-side management (DSM) are crucial for maintaining the balance between electricity supply and demand, as well as for peak shaving and valley filling. To support dual-carbon goals and enhance the economic efficiency of smart grids, this paper proposes a social welfare-maximising model that considers the interests of both consumers and suppliers. The model aims to maximise consumer utility while minimising supply-side costs, accounting for spinning reserve constraints in thermal power generation, and integrating a tiered carbon trading mechanism to encourage low-carbon energy transitions. To address the non-smooth and discontinuous characteristics of tiered carbon trading costs, a smoothing transformation is introduced to improve numerical tractability and algorithmic stability. A distributed optimisation dispatch method using an improved Alternating Direction Method of Multipliers (ADMM) is employed for the solution. Finally, the convergence and effectiveness of the proposed algorithm are verified through simulation results. Compared to the traditional ADMM algorithm, the proposed adaptive step-size ADMM significantly improves convergence efficiency, reducing the number of iterations required for primal residual convergence from 83 to 39 and for pairwise residuals from 84 to 45, while enhancing computational stability.*

Keywords: *smart grid, Demand side management (DSM), stepwise carbon trading, Real-time pricing (RTP), Alternating Direction Multiplier Method (ADMM).*

JEL Classification: Q41, Q48, D61.

Received: 3 August 2025	Revised: 7 January 2026	Accepted: 5 March 2026

1. Introduction

With the globalisation of the economy and rising energy demand, the global energy landscape is shifting toward a safer, more efficient, and lower-carbon structure (Xiong et al., 2023). The growing penetration of renewable energy brings inherent intermittency and variability, significantly affecting optimal smart grid configuration (Gao, 2022). Smart grids, valued for enhancing user convenience and

DOI: 10.24818/18423264/60.1.26.05

reducing carbon emissions, have developed rapidly but face challenges in managing load fluctuations (Amadeh et al., 2022).

Demand-side management (DSM), as a key regulatory mechanism, facilitates renewable integration, peak shaving, valley filling, and supply–demand balance, thereby improving energy utilisation and socio-economic benefits (Nan et al., 2023)). Among DSM strategies, real-time pricing (RTP) based on demand response is considered the most effective, with price responsiveness as its core (Wu et al., 2023). RTP adjusts electricity prices in real time to reflect the marginal value of electricity, while demand response (DR) programs actively optimise consumption, addressing operational and reliability issues in electricity markets (Sharma et al., 2021). This approach enhances the economic efficiency of providers and enables consumers to make informed energy decisions, balancing the interests of both sides (Deng et al., 2015).

Research on RTP strategies mainly develops along two perspectives. The first perspective regards electricity as a public good, aiming to maximise social welfare. Samadi et al. (2010) first proposed a model that maximises the difference between total user utility and supplier cost. Building on this, later studies introduced more realistic considerations, such as appliance categorisation (Li, Pan, & Gao, 2020), user classification (Wu et al., 2021), stochastic user responses (Tao et al., 2019), and time-coupled constraints (Tao & Gao, 2020). To address the limitations of static demand functions, dynamic demand response models have also been explored. For example, Fleuschutz et al. (2021) analysed the impact of price-based demand response on carbon emissions in European markets, providing a more accurate reflection of user behaviour and environmental effects.

The second perspective focuses on market mechanisms and adopts game theory to capture interactions between supply and demand. Game-theoretic methods are effective in modelling such strategic behaviours (Zhang et al., 2022). Representative works include Sun et al. (2023), who developed a leader–follower game framework considering user carbon quotas, and Yudong & Junjie (2023), who designed a two-stage Stackelberg model to optimise pricing and load adjustments. Zhang et al. (2022) further applied a bilevel stochastic model combined with multi-agent reinforcement learning to improve RTP through adaptive interactions between suppliers and consumers.

Many studies have addressed the diversity of power sources and the complementary nature of PV and wind power. To manage the randomness of renewable generation, Meng et al. (2022) proposed reserving spinning reserve to mitigate inaccurate wind forecasts. Zhang et al. (2022) investigated combining concentrating solar power and thermal power with electric heating to enhance spinning reserve in high-wind-power grids, optimising standby capacity to improve reliability. However, higher spinning reserve from thermal units increases carbon emissions. Li and Li (2023) incorporated a tiered carbon trading mechanism into the optimisation model, confirming its effectiveness in reducing emissions.

The stepwise carbon trading mechanism incentivises emission reduction by setting differentiated carbon prices, but its non-smooth, discontinuous nature

challenges optimisation algorithms like ADMM, which require smooth functions for efficient convergence. Yang et al. (2020) applied ADMM to handle renewable randomness and load uncertainty but did not address discontinuity in carbon trading. Zhang and Gao (2023) improved ADMM with an adaptive step-size for distributed optimisation, enhancing efficiency but overlooking tiered carbon trading complexities. Wu et al. (2023) extended ADMM to multi-variable convex problems and RTP strategies, resolving convergence issues, yet non-smoothness remained unaddressed. nevertheless, the applicability of their method is limited when facing discontinuous or non-smooth cost structures, such as those arising from tiered carbon trading mechanisms commonly adopted in low-carbon power systems.

This paper proposes a novel approach that smooths the discontinuous carbon trading mechanism for ADMM compatibility. By transforming the stepwise carbon trading cost into a continuously differentiable approximation, the proposed method effectively eliminates the numerical difficulties caused by non-smooth functions, thereby improving algorithmic stability and convergence behaviour in distributed optimisation. The developed social welfare maximisation model optimises both supply-side and consumer interests, integrates the stepwise carbon trading mechanism with smoothed costs, considers renewable uncertainty, and includes spinning reserve requirements for thermal generators. An enhanced adaptive step-size ADMM algorithm is used for distributed optimisation. Simulation results confirm the model's effectiveness and practical value.

The remainder of this paper is organised as follows. Section 2 presents the system model, including the stepwise carbon trading mechanism, renewable energy uncertainty modelling, demand response formulation, and spinning reserve constraints. Section 3 introduces the solution methodology based on the adaptive step-size ADMM algorithm and details the algorithmic implementation. Section 4 provides simulation settings and numerical results to validate the effectiveness and convergence performance of the proposed approach. Finally, Section 5 concludes the paper and discusses key findings and practical implications.

2. System Model

To systematically address the social welfare maximisation problem, this section is structured into three logical layers. First, we define the objective functions, including the stepwise carbon trading model (Section 2.1) and the individual costs/utilities of the stakeholders (Sections 2.2–2.5). Second, we establish the physical and operational constraints, such as supply-side costs and spinning reserves (Sections 2.6–2.8). Finally, the comprehensive social welfare model is formulated in Section 2.9, providing a rigorous mathematical basis for the distributed optimisation in the subsequent section.

The power system considered includes both suppliers and users. There are two types of suppliers: thermal power generation and wind and PV power generation. An electricity consumption period is divided into t slots, with T being the set of these time slots, $T = \{1,2,\dots,t\}$, The set of users is represented by $i = \{1,2,\dots,N\}$, the set

of thermal power generators by $J = \{1,2,\ldots,j\}$, the set of wind power generators by $M = \{1,2,\ldots,m\}$, and the set of PV power generators by $S = \{1,2,\ldots,s\}$.

2.1 Stepwise carbon trading mechanism

In carbon trading, emission rights are treated as tradable commodities. Power sources adjust their day-ahead dispatch according to allocated quotas. Excess emissions must be purchased, while surplus can be sold. In China, quotas are mainly gratuitous, especially for thermal power generators, as defined by Li et al. (2020).

$$E_q = \varepsilon \sum_{t\in T} P_T^t \tag{1}$$

Where P_T^t is the output power of the thermal power generator units, ε is the emission quota per unit of electricity, which is obtained by the weighted average of the marginal emission factor of electricity and the marginal emission factor of capacity. Following the mathematical framework presented in Zhang et al. (2025), a stepwise carbon trading mechanism is employed to further incentivise emission reduction. This model imposes incremental unit costs as emissions exceed progressively higher thresholds, as shown in the following equation.

$$E_R = \sum_{t\in T}(\alpha_j + \beta_j P_T^t + \gamma_j (P_T^t)^2) \tag{2}$$

Where α_j, β_j and γ_j are the carbon emission coefficients.

To more effectively regulate total carbon emissions, a stepwise carbon trading model is proposed, where the carbon trading cost is formulated as described by Meng et al. (2022), carbon trading cost is represented as

$$(E_R) = \begin{cases} \delta\left(E_R - E_q\right) & E_R \le l_c + E_q \\ \delta(1+\theta)\left(E_R - E_q - l_c\right) + \delta l_c & l_c + E_q < E_R \le 2l_c + E_q \\ \delta(1+2\theta)\left(E_R - E_q - 2l_c\right) + (2+\theta)\delta l_c & 2l_c + E_q < E_R \end{cases} \tag{3}$$

Where $C(E_R)$ is the stepwise carbon trading cost. A positive value indicates that carbon emissions have exceeded the allocated quota at a given time, which requires the purchase of additional allowances from the carbon trading market. Conversely, a negative value signifies that the allocated carbon quota has not been fully utilised, allowing the surplus to be sold for profit. δ、l are the carbon trading price and the length of the carbon emission volume interval; θ is the multiplier of the carbon trading price for each incremental unit of the tiered carbon emission volume.

The function is smooth when $E_R \neq l_c + E_q$、$E_R \neq 2l_c + E_q$、$E_R \neq 3l_c + E_q$、$E_R \neq 4l_c + E_q$, but it is non smooth when $E_R = l_c + E_q$、$E_R = 2l_c + E_q$、$E_R = 3l_c + E_q$、$E_R = 4l_c + E_q$. For the convenience of representation, set $C(E_R)_1 = \delta\left(E_R - E_q\right), C(E_R)_2 = \delta(1+\theta)\left(E_R - E_q - l_c\right) + \delta l_c, C(E_R)_3 = \delta(1+2\theta)\left(E_R - E_q - 2l_c\right) + (2+\theta)\delta l_c$the smooth approximation set of the cost of stepwise carbon trading can be approximated as

$$C(E_R)_\tau = \frac{C(E_R)_1 + \sqrt{C(E_R)_1 - C(E_R)_1^2 + 4\tau^2}}{4} + \frac{C(E_R)_3 + \sqrt{C(E_R)_3 - C(E_R)_2^2 + 4\tau^2}}{4} \tag{4}$$

Where $\tau \neq 0$ is a smooth parameter, when $\tau \neq 0$, $C(E_R)_\tau$ is smooth, and when$\tau = 0$, $C(E_R)_\tau = C(E_R)$.

2.2 Uncertain modelling of wind and solar power

The randomness of wind power generation depends on the wind speed changes. The available power for the t time slot is defined as p_{WT}^t, and the relationship between wind power output and wind speed is expressed as discussed by Sun, Li, Hu, et al. (2023)

$$P_{WT}^t = \begin{cases} P_r^t & v_r < v_t < v_{\text{co}} \\ P_r^t \frac{v_t - v_{\text{ci}}}{v_r - v_{\text{ci}}} & v_{\text{ci}} < v_t < v_r \\ 0 & v_t \leq v_{\text{ci}}, v_t \geq v_{\text{co}} \end{cases} \tag{5}$$

Where v_{ci}、v_{co}、v_r、v_t are the cutting in and cutting out speeds, rated wind speed, and wind speed at t time slot of the wind turbine; P_r^t is the rated output power of the wind power; P_{WT}^t is the wind power output power at t time slot.

The wind speed follows a Weibull distribution, and the probability distribution is expressed as

$$f(v_k) = \frac{k_s}{c}\left(\frac{v_k}{c}\right)^{k_s - 1} exp\left[-\left(\frac{v_k}{c}\right)^{k_s}\right] \tag{6}$$

Where k_s and c are the shape and scale parameters of the Weibull distribution, PV are related to solar radiation, and the output model of PV generators is represented as

$$P_{PV}^t = P_{PVR}\frac{G(t)}{G_R}[1 + \tau(T(t) - T_R)] \tag{7}$$

Where G_R and $G(t)$ are the rated light radiation and the light radiation at t time slot; T_R and $T(t)$ are the rated temperature and the temperature at t time slot; $P_{PVR}$is the rated output power of the PV system; P_{PV}^t is the PV output power at t time slot; τ is the actual lighting intensity.

The light intensity follows a Beta distribution, and the probability distribution is expressed as

$$f\left(\frac{P_{PV,s}^t}{P_{PVR}}\right) = \frac{1}{\Gamma(\alpha_s - \beta_s)}\left(\frac{P_{PV,s}^t}{P_{PVR}}\right)^{\alpha_s - 1} \times \left(1 - \frac{P_{PV,s}^t}{P_{PVR}}\right)^{\beta_s - 1} \tag{8}$$

Where $\Gamma(\cdot)$is the Gamma distribution; α_s and β_s are the shape parameter of the Beta distribution.

New energy power generation includes wind power generation and PV power generation, the total output power of new energy supply at t time slot is defined as

$$P_R^t = P_{WT}^t + P_{PV}^t \tag{9}$$

2.3 Demand Response Model Based on Elastic Matrix

The price elasticity of demand is defined as

$$E = \frac{\Delta d/d_o}{\Delta p/p_o} \tag{10}$$

where Δp is the demand, Δd is the change in price, p_0 and d_0 are the initial demand and electricity price. Using electricity price as the influencing factor for load forecasting and as the model input. The demand at a certain moment is not only related to the current electricity price, but also influenced by the electricity prices at other times. The elastic electricity price is expressed as

$$\Delta l_0 = E\,\frac{p(t)-p_0(t)}{p_0(t)} \tag{11}$$

where $p(t)$ is the unit electricity price of the user at t time slot, and $p_0(t)$ is the initial unit electricity price.

The demand of users at t time slot under RTP is expressed as

$$P\left(x_i^t\right) = P_0\left(x_i^t\right) + \left[1 + E\,\frac{p(t)-p_0(t)}{p_0(t)}\right] \tag{12}$$

After implementing RTP, it should be ensured that the electricity expenditure of users cannot exceed the expenditure before implementing demand response, expressed as

$$\beta \sum_{k\in K} p_0(t) P\left(x_i^t\right) \geq \sum_{k\in K} p(t) P\left(x_i^t\right) \tag{13}$$

where P_0 is the user's initial electrical energy, by setting different scaling factors β Value that can adjust the user's electricity expenditure.

2.4 Spinning reserve constraints for thermal generators

The output constraint of a thermal power generator is expressed as formulated by Zhang et al. (2022)

$$\begin{cases} P_T^{t,min} \leq P_T^t \leq P_T^{t,max} \\ P_{WT}^{t,min} \leq P_{WT}^t \leq P_{WT}^{t,max} \\ P_{PV}^{t,min} \leq P_{PV}^t \leq P_{PV}^{t,max} \end{cases} \tag{14}$$

Where $P_{\mathrm{T}}^{\mathrm{t,max}}$,$P_{\mathrm{T}}^{\mathrm{t,min}}$ are the upper and lower limits of the output of the thermal power generation unit at t time slot; $P_{\mathrm{WT}}^{\mathrm{t,max}}$、$P_{\mathrm{WT}}^{\mathrm{t,min}}$are the upper and lower limits of the output of the wind turbine at t time slot; $P_{\mathrm{PV}}^{\mathrm{t,max}}$,$P_{\mathrm{PV}}^{\mathrm{t,min}}$ are the upper and lower limits of the output of the PV generator set at t time slot.

Thermal power units can reserve a certain amount of spinning reserve to cope with the uncertainty of wind power generation, so that they can compensate for the uncertainty of new energy generation within a certain level of confidence, expressed as

$$\begin{cases} P_T^t + R_{i,t}^u \le P_T^{t,max} \\ \sum_{m\in M} R_{i,t}^u \le R_{i,t}^{\mathrm{u,max}} \\ P_T^t - R_{i,t}^u \ge P_T^{t,min} \\ \sum_{m\in M} R_{i,t}^d \ge R_{i,t}^{\mathrm{d,max}} \end{cases} \tag{15}$$

Where $R_{i,t}^u$ and $R_{i,t}^d$ is the up and down rotation backup; $R_{i,t}^{u,max}$ and $R_{i,t}^{d,max}$ is the lower and upper limits of climbing constraints for thermal power units.

2.5 Wind power deterministic Constraints

Consider providing a certain amount of up and down rotation backup through thermal power units that can meet the deviation between the rated output power of wind power$P_r^t$and the output power of wind powerP_{WT}^twithin a certain confidence level, deterministic Constraints described as

$$\begin{aligned} &Pr\{\textstyle\sum_{j\in J}(P_r^t - P_{WT}^t) \le \sum_{s\in S} R_{i,t}^u\} \ge c^+ \\ &Pr\{\textstyle\sum_{j\in J}(P_{WT}^t - P_r^t) \le \sum_{s\in S} R_{i,t}^d\} \ge c^- \end{aligned} \tag{16}$$

Where$c^+$and$c^-$are the confidence levels for the up and down rotation reserve.

2.6 Power generation cost function

The cost function of thermal power generation is a strictly convex function, using a quadratic function as the cost function. The cost function of thermal power generation considering carbon trading costs is represented as proposed by Zhang et al. (2022)

$$C(P_T^t) = a_T(P_T^t)^2 + b_T P_T^t + c_T + G_T P_T^t e_T + C(E_R) \tag{17}$$

Where a_{T},b_{T},c_{T} are the combustion coefficient of thermal power units, G_{T} is the environmental cost parameters for pollutants generated by thermal power generators; e_{T} is the environmental cost parameters for unit power generation pollution.

When power generation exceeds load demand, situations of "curtailed wind and solar power" occur. The randomness of wind and solar power generation can lead to underestimation and overestimation of actual electricity usage. Considering the penalty costs for overestimations and underestimations caused by the uncertainty of new energy generation, the cost of new energy generation is given as

$$C(P_R^t) = \textstyle\sum_{m\in M} m_{wt} P_{WT}^t + \sum_{s\in S} n_{pv} P_{PV}^t + d_{WT}^{ue} E(Y_{WT}^{t,ue}) + d_{WT}^{oe} E(Y_{WT}^{t,oe}) \tag{18}$$

Where $E(Y_{\mathrm{WT}}^{\mathrm{t,ue}})$ and $E(Y_{\mathrm{WT},k}^{\mathrm{t,oe}})$ are the expected values for underestimation and overestimation of wind power generation, respectively. The first term represents the direct cost of wind power generation with a cost coefficient m_{wt}; the second term represents the direct cost of PV power generation with a cost coefficient n_{pv}; the third term represents the penalty cost for underestimating wind power generation, which penalises for scheduling less wind energy than what is actually used, with a

cost coefficient d_{WT}^{ue}; and the fourth term represents the penalty cost for overestimating wind power generation, which penalises for actual use of wind energy being less than the scheduled wind energy, with a cost coefficient d_{WT}^{oe}.

2.7 Utility Function

The utility function reflects users' satisfaction as electricity consumption changes. It is non-decreasing and concave, with diminishing marginal utility, allowing satisfaction to gradually saturate. The utility function is adopted from Deng et al. (2015).

$$U(x,\omega)=\begin{cases}\omega x-\frac{\alpha}{2}x^2 & 0\le x\le\frac{\omega}{\alpha}\\ \frac{\omega^2}{2\alpha} & x\ge\frac{\omega}{\alpha}\end{cases} \tag{19}$$

Where x is the electricity consumption; $\alpha\in(0,1)$ is a predetermined parameter, set in advance based on each user's electricity usage situation; $\omega>0$ is a parameter reflecting the user utility situation, which varies from user to user. The utility function for user i at t time slot can be expressed as $U\left(x_i^t,\omega_i^t\right)$.

2.8 Transformation of Stochastic Constraints to Deterministic Constraints

By introducing the cumulative distribution function of wind power, the stochastic constraint (15) is transformed into a deterministic linear constraint. The distribution function for wind power is

$$F_{P_r^t}(P_{WT}^t)=\begin{cases}0 & P_{WT}^t<0\\ 1-exp\left(-\left(\frac{v_{ci}+\frac{P_{WT}^t}{P_r^t}v_{ci}}{c}\right)^k\right) & 0<P_{WT}^t<P_r^t\\ +exp\left(-\left(\frac{v_{co}}{c}\right)^k\right) & \\ 1 & P_r^t\le P_{WT}^t\end{cases} \tag{20}$$

From this, the inverse function $F_{P_r^t}^{-1}(P_{WT}^t)$ of $F_{P_r^t}(P_{WT}^t)$ is derived as

$$F_{P_r^t}^{-1}(P_{WT}^t)=\begin{cases}-\infty & c^-=0\\ \frac{P_r^t c}{v_r-v_{in}}\left(-In\left(1+exp\left(-\left(\frac{v_{out}}{c}\right)^k\right)\right)-c^-\right)^{\frac{1}{k}}-\frac{P_r^t}{h} & 0<c^-<1\\ +\infty & c^-=1\end{cases} \tag{21}$$

Where$h=\frac{v_r}{v_{in}}-1$, The inverse function of the cumulative distribution function of P_r^t represented by a $F_{P_r^t}^{-1}(\cdot)$

According to the above inverse function, the Deterministic Constraints can be transformed into the following deterministic inequality constraint, which can be transformed into

$$\begin{aligned}&\sum_{j\in J} P_r^t - \sum_{s\in S} R_{i,t}^u \le F_{P_r^t}^{-1}(1-c^+)\\ &\sum_{j\in J} P_r^t + \sum_{s\in S} R_{i,t}^d \ge F_{P_r^t}^{-1}(c^-)\end{aligned} \tag{22}$$

For the convenience of subsequent calculations, the model is evolved by defining auxiliary vectors for local decision variables for each generator set l as

$$x_{l,t} = \begin{cases}\left[P_T^t, R_{i,t}^u, R_{i,t}^d\right] & l \in \{1,\dots,j\}\\ P_R^t & l \in \{j+1,\dots h\}\end{cases} \tag{23}$$

Represent the coupling inequality (22) in matrix form as

$$\sum_{h\in H} A_l x_{l,t} \le \tilde{b} \tag{24}$$

When $\tilde{b} = \left[F_{P_r^t}^{-1}(1-c^+), F_{P_r^t}^{-1}(c^-)\right]$, $A_l = \begin{cases}\begin{bmatrix}0 & -1 & 0\\ 0 & 0 & -1\end{bmatrix} & l \in \{1,\dots,j\}\\ [1,-1]^T & l \in \{j+1,\dots h\}\end{cases}$

By introducing the relaxation variable $s_{l,t}$, we transform the linear matrix inequality as

$$\sum_{h\in H}\left(A_l x_{l,t} + s_{l,t}\right) = \tilde{b}, 0 \le s_{l,t} \le \bar{s} \tag{25}$$

Where $\bar{s}$ satisfies $\bar{s} \ge \tilde{b}$, it is a constant vector with the same dimension as $\tilde{b}$, represented in set form $S_{l,t} = \{s_{l,t} | 0 < s_{l,t} < \bar{s}\}$, order $\mu_{l,t} = \left[x_{l,t}, s_{l,t}\right]$, which can be expressed as

$$\sum_{h\in H} A_l \mu_{l,t} = \tilde{b} \tag{26}$$

Where $\tilde{A}_l = [A_l, I]$, I is a four-dimensional identity matrix.

For any scheduling period, the total scheduling power output of thermal and wind power units needs to meet the total load demand, and the power balance constraint is expressed as

$$\sum_{h\in H} E_l x_{l,t} = \sum_{i\in N} P\left(x_i^t\right) \tag{27}$$

where

$$E_l = \begin{cases}[1,0,0] & l \in \{1,\dots,J\}\\ 1 & l \in \{j+1,\dots,H\}\end{cases} \tag{28}$$

Similarly, equations (26) and (27) can be represented as

$$\sum_{h\in H} \tilde{E_l} \mu_{l,t} = \tilde{b} \tag{29}$$

Where $\tilde{E}_l = [E_l, 1]$, 1 is a column vector that represents four dimensions and all elements are one.

2.9 Maximising social welfare model

Equations (13) and (14) can be considered as auxiliary constraints. In the consumption process of the electricity market, the optimisation problem can be decomposed and solved independently for each time slot k∈K. When k∈K is fixed, the maximisation of social welfare can be transformed into a problem that only considers the maximisation of social welfare for a certain time period. The smart grid

RTP model considering the maximisation of social welfare as described by Taoet al. (2019)

$$max\, W_{l,t}\left(\mu_{l,t}\right) = \sum_{i\in N}\left(U\left(P\left(x_i^t\right),\omega_i^k\right) - C\left(P_T^t\right) - C\left(P_R^t\right)\right)$$

$$s.t.\sum_{h\in H}\tilde{E}_l\mu_{l,t} = \tilde{b} \tag{30}$$

3. Algorithm Solution

3.1 Principle of ADMM Algorithm

The core of ADMM is to decompose complex problems into sub-problems, iteratively update variables and dual variables until convergence. It is effective for convex optimisation with equality constraints (Zhang & Gao, 2023).

$$\begin{aligned} &min\, f\,(x) + g(z) \\ &s.t.\, Ax_s + Bz_s = b \end{aligned} \tag{31}$$

Where $f(x)$ and $g(x)$ are the two subproblems decomposed into the objective function, x and z are the variable vectors in$f(x)$ and $g(x)$; X_S and Z_S are shared variable vectors in $f(x)$ and $g(x)$; A、B and b are the coefficient matrices of the coupling relationship between shared variables. The augmented Lagrangian function is represented as formulated by Zhang and Gao (2023)

$$L(x,y,z,\lambda) = f(x) + g(y) + h(z) - \lambda(Ax + By - Cz - b) + \frac{\rho}{2}\|Ax + By - Cz - b\|_2^2 \tag{32}$$

Where x、y and z are separable operator, A、B and C are parameters， λ is a multiplier variable, ρ is a penalty factor and a constant.

$$\begin{cases} x^{k+1} = argminL(x,z^k,\lambda^k) \\ z^{k+1} = argminL(x^k,z,\lambda^k) \\ \lambda^{k+1} = \lambda^k - \rho(A^{k+1} + Cz^{k+1} - b) \end{cases} \tag{33}$$

The superscript k、$k+1$ in the formula represent the values after the k and $k+1$ iterations; $argmin(\cdot)$ is the value of the independent variable when obtaining the minimum value.

3.2 Adaptive step-size ADMM

The adaptive step-size ADMM improves the traditional ADMM by automatically updating the step size during iterations, enhancing convergence and computational efficiency. The Lagrangian function for Problem (31) is defined as

$$L\left(\mu_{l,t},\lambda_{l,t}\right) = W_{l,t}\left(\mu_{l,t}\right) + \lambda_{l,t}^T\left(\sum_{h\in H}\tilde{E}_l\mu_{l,t} - \tilde{b}\right) + \frac{\rho}{2}\left\|\sum_{h\in H}\tilde{E}_l\mu_{l,t} - \tilde{b}\right\|^2 \tag{34}$$

Where λ_t is a dual variable; ρ is the penalty factor and is constant. According to the ADMM algorithm, there are

$$\mu_{l,t}^{k+1} = argmin\begin{pmatrix} L\left(\mu_{l,t},\lambda_{l,t}\right) + \lambda_{l,t}^k\left(\tilde{E}_l\mu_{l,t} - \tilde{b}\right) \\ +\frac{\rho}{2}\left\|\sum_{h\in H}\tilde{E}_l\mu_{l,t} - \tilde{b}\right\|^2 \end{pmatrix} \tag{35}$$

$$d_{l,t}^{k+1} = \frac{1}{H}\sum_{h\in H}\left(\mu_{l,t}^{k+1} + \frac{1}{\rho}\lambda_{l,t}^{k+1}\right) \tag{36}$$

$$\lambda_{l,t}^{k+1} = \lambda_{l,t}^{k} + \rho\left(\mu_{l,t}^{k+1} - d_{l,t}^{k+1}\right) \tag{37}$$

Where ρ is a constant penalty factor. $d_{l,t}^{k+1}$ is the consensus global variable.

The calculation method for original residual and dual residual is presented by Zhang and Gao (2023)

$$\begin{cases} \left\|\mu_{l,t}^{k+1} - \mu_{l,t}^{k}\right\| \le \delta^{pri} \\ \left\|\lambda_{l,t}^{k+1} - \lambda_{l,t}^{k}\right\| \le \delta^{dual} \end{cases} \tag{38}$$

Where δ^{pri} and δ^{dual} are the upper tolerance limits for the original residual and the dual residual.

3.3 Model solving

In traditional ADMM, the selection of the penalty parameter (step size) ρ is critical; an excessively large ρ can lead to slow convergence by over-penalising primal residuals, while an improperly small ρ may cause numerical instability or even divergence in non-convex scenarios. As demonstrated by Boyed et al. (2010). and further analysed in smart grid applications, an adaptive step-size mechanism is essential to balance the convergence of primal and dual residuals dynamically.

$$\rho^{k+1} = \begin{cases} \frac{\rho^{k}}{1+lg\left(\delta^{pri}/\delta^{dual}\right)} & \delta^{pri} < 0.1\delta^{dual} \\ \rho^{k}\left[1 + lg\left(\delta^{pri}/\delta^{dual}\right)\right] & \delta^{dual} < 0.1\delta^{pri} \\ \rho^{k} & other \end{cases} \tag{39}$$

The above adaptive adjustment mechanism can balance the convergence speed of the primal residual and the dual residual, preventing either from converging too slowly. When the primal residual δ^{pri} is relatively large, the step size is increased, i.e., the proportion of the norm term in (39) is increased to accelerate the convergence of the primal residual δ^{pri}; when the primal residual δ^{pri} is relatively small, reducing the step size can decrease the oscillation of the objective function. To implement this adaptive step-size strategy, the following computational procedure is adopted.

Adaptive Step-Size ADMM

Step 1 For nodes $l\{1,\ldots,J\}, l\{1,\ldots,H\}$, initialize$\tilde{E}_l, \tilde{b}$;

Step 2 Set parameters (including carbon trading market price, new energy parameters, etc.);

Step 3 Input initial values of $P(x_i^t)$,P_T^k, P_{WT}^k, P_{pv}^t and the Lagrangian dual variable $\lambda_t \in (0,1)$;

Step 4 Alternate computation according to equations (35), (36), and (37);

Step 5 Convergence judgment, end computation if termination conditions (i.e., convergence of primal and dual residuals) are satisfied; otherwise, set $k = k + 1$ and return to Step 4.

4. Simulation

4.1 Simulation Environment and Parameter Configuration

To evaluate the performance of the proposed adaptive step-size ADMM strategy, a simulation is conducted based on a smart grid scenario consisting of 3 thermal power plants, 4 wind power plants, and 4 PV power plants serving 100 users. The day is divided into 24 one-hour time periods. The operational parameters for the thermal units, including the cost coefficients a_T, b_T, and c_T, are selected based on the standard IEEE test systems and adjusted according to the empirical data presented by Zhang et al. (2022), as detailed in Table 1.For the carbon trading mechanism, the baseline quota l_c is set to 9000, with a carbon trading price interval δ of 0.25 and a price growth rate θ of 0.25. These parameters are chosen in alignment with the current carbon market policies in China, as discussed by Zhang et al. (2025) to ensure the practical relevance of the simulation. To ensure an unbiased comparison, the initial step size for the traditional ADMM is set to the optimal fixed value obtained through sensitivity pre-tests, following the benchmarking approach suggested by Boyd et al. (2011).

Table 1. Parameters of thermal generator

Unit number	a_T	b_T	c_T	G_T	e_T
1	0.02	2	90	0.3	0.918
2	0.015	1.95	80	0.3	0.934
3	0.01	1.75	100	0.3	0.855

Source: Authors' own processing.

4.2 Result simulation

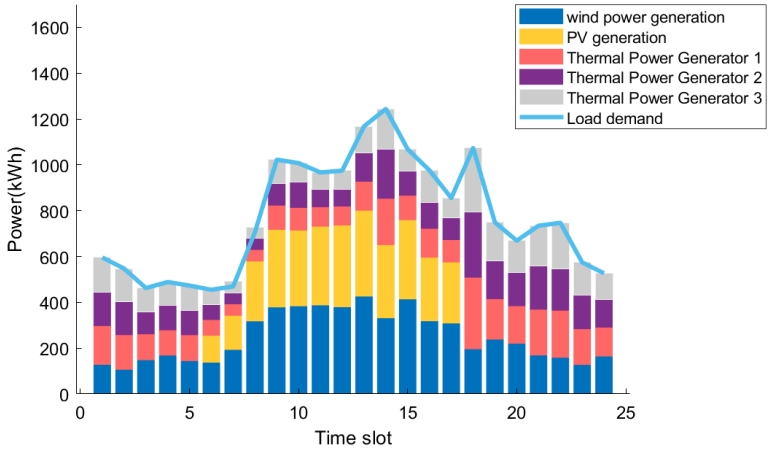

Figure 1. Load situation and load demand curve
Source: Authors' own creation.

Figure 1 shows the overall load and the generation from wind, PV, and thermal sources. Renewable generation peaks between 07:00 and 17:00, contributing significantly to total supply. The load is lowest from 00:00 to 07:00, peaks from 07:00 to 20:00, and then declines until 24:00. Total generation meets the load demand, minimising curtailment and ensuring efficient energy use.

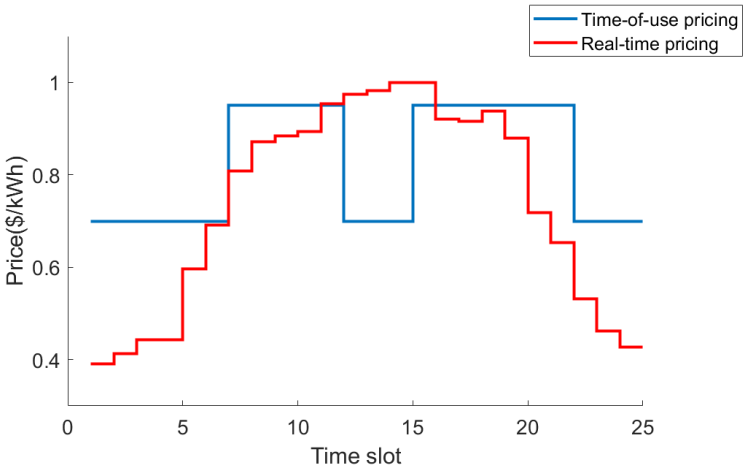

Figure 2. 24-hour RTP tariffs and TOU tariffs
Source: Authors' own creation.

Figure 2 presents the RTP and TOU tariffs over a full day. RTP closely follows fluctuations in load demand: prices rise during peak hours to reflect higher demand, and fall during off-peak hours to encourage consumption. This dynamic pricing mechanism balances supply and demand while promoting more efficient energy use.

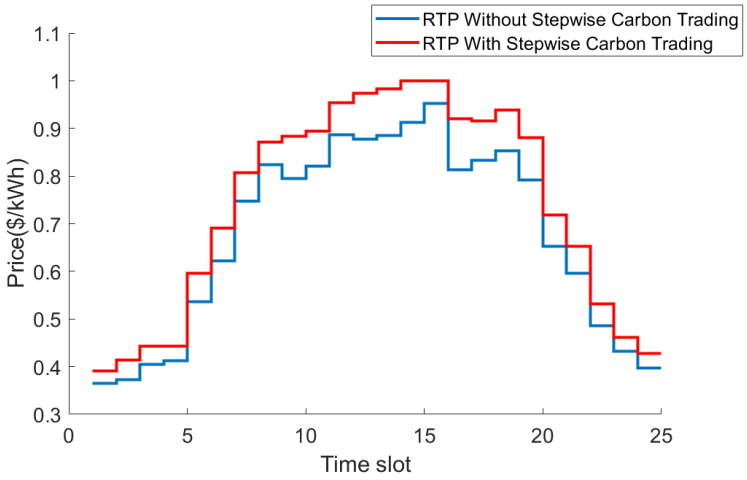

Figure 3. Impact of Stepwise Carbon Trading on RTP
Source: Authors' own creation.

Figure 3 shows that stepwise carbon trading results in sharper RTP increases during peak hours (08:00-22:00) compared with the smoother pattern under non-stepwise carbon trading. The tiered carbon cost mechanism causes noticeable price jumps in high-emission periods, reflecting the added cost of carbon allowances.

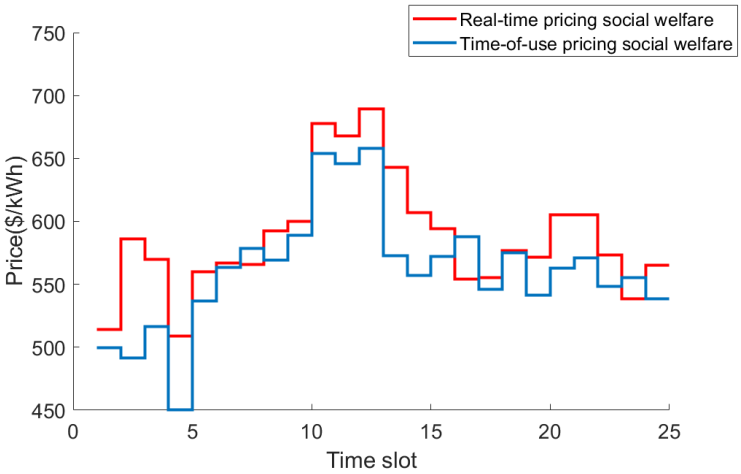

Figure 4. Comparison of 24-hour social welfare
Source: Authors' own creation.

Figure 4 compares social welfare under RTP and TOU tariffs. RTP outperforms TOU from 06:00-22:00, especially between 10:00 and 22:00, while TOU is slightly higher overnight. Overall, RTP achieves greater total social welfare.

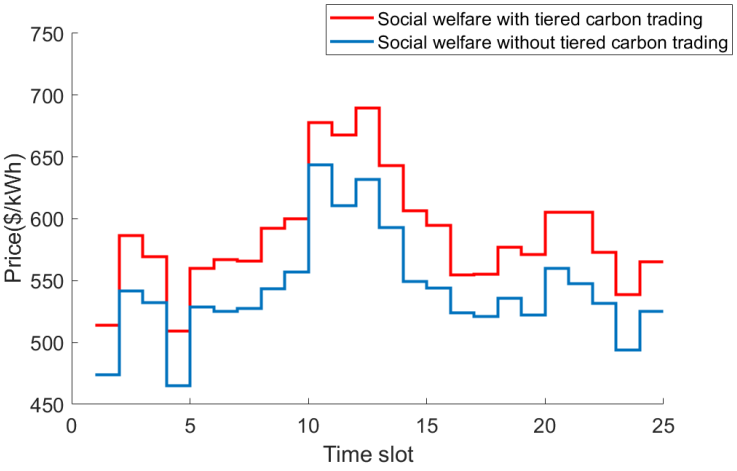

Figure 5. Comparison of Social Welfare with and without Tiered Carbon Trading
Source: Authors' own creation.

Figure 5 indicates that introducing tiered carbon trading generally increases social welfare throughout the day. This is mainly due to higher electricity prices boosting supplier revenue, while consumer participation remains robust, showing the mechanism's effectiveness in enhancing market efficiency.

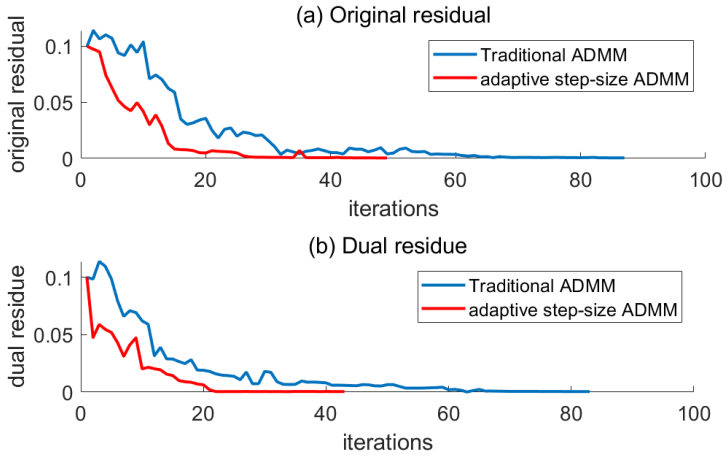

Figure 6. Convergence Performance of Traditional ADMM vs. Adaptive Step-Size ADMM
Source: Authors' own creation.

Figure 6 compares the convergence performance of the traditional ADMM algorithm and the adaptive step-size ADMM algorithm. The results show that the original residuals in the traditional ADMM algorithm decrease slowly, requiring 83 iterations to reach a convergence accuracy of 5×10^{-4}, whereas the improved algorithm achieves the same accuracy in just 39 iterations. Similarly, the pairwise residuals in the traditional ADMM algorithm take 84 iterations to converge to 5×10^{-4}, while the improved algorithm reaches this accuracy in only 45 iterations, demonstrating significantly enhanced convergence efficiency. This significant enhancement in efficiency is attributed to the adaptive mechanism, which dynamically balances the primal and dual residuals by adjusting the penalty parameter ρ. This approach avoids the convergence delays often caused by poorly selected fixed step sizes in traditional ADMM, demonstrating the robustness of the proposed strategy in complex scheduling scenarios.

5. Conclusions

Although the proposed model effectively addresses the stepwise carbon trading cost, certain limitations remain. First, this study assumes a deterministic environment for renewable energy output; however, in practice, the uncertainty of wind and solar power could affect the real-time pricing stability. Second, the model

currently focuses on a single-area grid, while multi-area interconnected scenarios require further investigation.

The RTP tariff in smart grids is an effective tool for peak shaving and valley filling. This paper considers stepped carbon trading and renewable uncertainties, proposes an RTP model aimed at maximising social welfare, and solves it using adaptive step-size ADMM. Simulation results confirm the model's feasibility, leading to the following conclusions:

(1) The social welfare maximisation model can effectively ensure the balance of supply and demand in the power system and the interests of the users and the supply side, and the RTP tariff can generate higher social welfare compared with theTOU tariff.

(2) The adaptive step-size ADMM algorithm can converge to the global optimal solution of the system within a certain error requirement and a limited number of iterations, which effectively solves the barriers of information and other aspects between different subproblems.

(3) The introduction of the tiered carbon trading mechanism significantly enhances social welfare by optimising electricity pricing. It provides stronger incentives for demand-side management and renewable energy adoption, leading to more efficient resource allocation and greater economic benefits.

References

[1] Amadeh, A., Lee, Z.E., Zhang, K.M. (2022), *Quantifying demand flexibility of building energy systems under uncertainty. Energy*, 246.

[2] Boyd, S., Parikh, N., Chu, E., Peleato, B., Eckstein, J. (2010), *Distributed Optimization and Statistical Learning via the Alternating Direction Method of Multipliers. Foundations & Trends in Machine Learning,* 3(1), 1-122.

[3] Deng, R., Yang, Z., Hou, F. (2015), *Distributed Real-Time Demand Response in Multiseller–Multibuyer Smart Distribution Grid. IEEE Transactions on Power Systems*, 30(5), 2364-2374.

[4] Fleuschutz, M., Bohlayer, M., Braun, M., Henze, G., Murphy, M.D. (2021), *The effect of price-based demand response on carbon emissions in European electricity markets. Applied Energy*, 295, 117014.

[5] Gao, Y. (2022), *A review on real-time electricity price optimisation methods based on demand side management. University of Shanghai for Science and Technology*, 002, 044.

[6] Li, J., Li, X. (2023), *Operation optimal strategy of community integrated energy Stackelberg game considering carbon trading. Power Demand Side Management*, 25(6), 28-34.

[7] Li, J.X., Pan, T.T., Gao, Y. (2020), *Real-time pricing algorithm for supply and demand of complementary energy on smart grid. Application Research of Computers*, 37(04), 1092-1096.

[8] Meng, L.Z.C., Yang, X.Y., Zhao, Z.Y. (2022), *An Economic Optimal Dispatch Strategy for Active Distribution Networks Considering Photovoltaic-Load Uncertainty and Rotating Reserve Constraints. Electric Power Construction*, 43(11), 63-72.

[9] Nan, B., Dong, S.F., Tang, K.J. (2023), *Optimal Configuration of Energy Storage in PV-storage Microgrid Considering Demand Response and Uncertainties in Source and Load. Power System Technology*, 47(4), 1340-1352.

[10] Samadi, P., Mohsenian-Rad, A.H., Schober, R., Wong, V.W.S., Jatskevich, J. (2010), *Optimal Real-Time Pricing Algorithm Based on Utility Maximization for Smart Grid. In 2010 First IEEE International Conference on Smart Grid Communications. IEEE.*

[11] Sharma, A.K., Saxena, A., Palwalia, D.K. (2021), *Supervised learning-based demand response simulator with incorporation of real time pricing and peak time rebate. International Transactions on Electrical Energy Systems,* 31.

[12] Sun, Y., Li, F., Hu, Y.J. (2023), *Energy Sharing Incentive Strategy of Prosumers Considering Conditional Value at Risk and Integrated Demand Response,* 38(9), 2448-2463.

[13] Tao, L., Gao, Y. (2020), *Real-time pricing for smart grid with distributed energy and storage: A noncooperative game method considering spatially and temporally coupled constraints. International Journal of Electrical Power & Energy Systems*, 115, 105487.

[14] Tao, L., Gao, Y., Zhu, H., Liu, S. (2019), *Distributed genetic real-time pricing for multiseller-multibuyer smart grid based on bilevel programming considering random fluctuation of electricity consumption. Computers & Industrial Engineering*, 135, 359-367.

[15] Wu, H., Ou, Y.S., Liang, W.K. (2023), *Distributionally robust optimisation configuration of photovoltaic-energy storage coordination in flexible distribution network based on adaptive step size ADMM. Electric Power Automation Equipment*, 43(7), 35-43.

[16] Wu, Z.Q., Gao, Y., Wang, B. (2021), *Real-time pricing strategy for the smart grid under "load-utility" two-level balance. Power System Protection and Control*, 49(17), 65-73.

[17] Wu, Z.Q., Wang, J.Q., Gao, Y. (2023), *Social Welfare Analysis of Real-time Pricing. Chinese Journal of Management Science*, 31(08), 1-10.

[18] Xiong, Z., Whang, S., Wang, L.L. (2023), *Robust Optimal Scheduling of Regional Integrated Energy System Considering Multi-Energy Flexibility Complementary and Users' Low-carbon Willingness. Power System Technology*, 47(11), 1-14.

[19] Yang, Z., Hu, J., Ai, X., Wu, J., Yang, G. (2021), *Transactive Energy Supported Economic Operation for Multi-Energy Complementary Microgrids. IEEE Transactions on Smart Grid*, 12(1), 4-17.

[20] Yudong, W., Junjie, H. (2023), *Two-stage energy management method of integrated energy system considering pre-transaction behavior of energy service provider and users. Energy*, 271.

[21] Zhang, L., Gao, Y., Zhu, H., Tao, L. (2022), *Bi-level stochastic real-time pricing model in multi-energy generation system: A reinforcement learning approach. Energy*, 239.

[22] Zhang, Y., Xia, S., Zhang, F. (2025), *The optimal allocation method of green power energy storage resources considering stepwise carbon trading. Journal of Physics: Conference Series*, 3096, 012001.

[23] Zhang, Y., Zhao, H., Li, B. (2022), *Research on dynamic pricing and operation optimisation strategy of integrated energy system based on Stackelberg game. International Journal of Electrical Power and Energy Systems,* 143, 108446.

[24] Zhang, Y.J., Gao, Y. (2023), *Real-Time Price Strategy Based on ADMM-GBS for Smart Grid Considering Wind and Solar Power Uncertainty. Distributed Energy*, 8(06), 27-35.

[25] Zhang, Y.X., Liu, W.Y., Pang, Q.L. (2022), *Optimal Power Spinning Reserve Method of Concentrating Solar Power and Thermal Power for High-Proportion Wind Power System. Transactions of China Electrotechnical Society*, 37(21), 5478-5489.